

# Anomalous transmission and drifts in one-dimensional Lévy structures

P. Bernabó<sup>a</sup>, R. Burioni<sup>b</sup>, S. Lepri<sup>c,d</sup>, A. Vezzani<sup>b,e</sup>

<sup>a</sup>Università degli Studi di Pisa, Dipartimento di Ingegneria dell'Informazione, Via G. Caruso 16 56122 - Pisa, Italy

<sup>b</sup>Università degli Studi di Parma, Dipartimento di Fisica, viale G.P. Usberti 7/A, 43100 Parma, Italy

<sup>c</sup>Consiglio Nazionale delle Ricerche, Istituto dei Sistemi Complessi, via Madonna del Piano 10, I-50019 Sesto Fiorentino, Italy

<sup>d</sup>Istituto Nazionale di Fisica Nucleare, Sezione di Firenze, via G. Sansone 1 I-50019, Sesto Fiorentino, Italy

<sup>e</sup>Consiglio Nazionale delle Ricerche, Centro S3, Istituto di Nanoscienze, Via Campi 213A, I-41125 Modena Italy

---

## Abstract

We study the transmission of random walkers through a finite-size inhomogeneous material with a quenched, long-range correlated distribution of scatterers. We focus on a finite one-dimensional structure where walkers undergo random collisions with a subset of sites distributed on deterministic (Cantor-like) or random positions, with Lévy spaced distances. Using scaling arguments, we consider stationary and time-dependent transmission and we provide predictions on the scaling behavior of particle current as a function of the sample size. We show that, even in absence of bias, for each single realization a non-zero drift can be present, due to the intrinsic asymmetry of each specific arrangement of the scattering sites. For finite systems, this average drift is particularly important for characterizing the transmission properties of individual samples. The predictions are tested against the numerical solution of the associated master equation. A comparison of different boundary conditions is given.

**Keywords:** Lévy walks; anomalous transport and diffusion; fractals; superdiffusive media; scaling; inhomogeneous disorder

---

## 1. Introduction

Transport and diffusion in complex systems is often anomalous, since the basic hypotheses underlying the laws of ordinary Brownian motion can be violated. Specific examples are abundant in physics and chemistry, ranging from porous media, to tracer motion in turbulent fluids and plasmas [1]. Interdisciplinary applications of non-Brownian processes also arised recently in diverse fields as animal movement [2] and social and cognitive phenomena [3]. In all these cases, the lengths of the steps taken by the diffusing particles can have large fluctuations, and typically follow a probability distribution with heavy tails.

Among the many possible experimental applications in physics, of special interest is the recent realization of materials termed Lévy glasses, where light rays propagate through an assembly of transparent spheres embedded in a scattering medium [4, 5]. If the diameter of spheres is designed to have a power-law distribution, light can indeed perform anomalous diffusion. From the theoretist viewpoint, a salient feature of such experiment is that the spatial arrangement of the scattering media is fixed for each sample, i.e. the disorder is quenched. This implies that the walk is correlated as light that has just crossed a large glass sphere has a larger probability of being backscattered at the following step and thus to perform a jump of roughly the same length.

The reference model for this class of phenomena is the so-called Lévy walk [6, 7, 8], in which particles perform in-

dependent steps  $l$  at constant velocity, with a distribution following an algebraic tail of the form  $l^{-(1+\alpha)}$  for large  $l$ . Such a heavy-tailed distribution arises in presence of dynamical correlations, like in the case of diffusion in chaotic and intermittent systems [9, 8], or from complex interaction with the environment [10, 11]. When the variance of  $l$  diverges, for  $\alpha < 2$ , transport is thereby dominated by very long steps, the mean square displacement increases faster than linearly with time, and transport is superdiffusive.

While the case of uncorrelated jumps (annealed) is well understood, quenching effects are known to affect strongly the diffusion properties [12, 13, 14] and in this case there are still many open problems. Relevant features of experiments on scattering in inhomogeneous media can be described as a random walk in a quenched, long-range correlated environments and can be studied directly by Monte Carlo simulations [15, 16]. However, simplified models are of great help to provide theoretical insight. In this context, a minimal model that includes the effects of disorder and anomalous diffusion consists of a free particle moving through a one-dimensional array of scatterers whose spacing is power-law distributed [17, 18, 19]. In this spirit, a closely related class of self similar models, termed Cantor graphs has been also considered [20]. As the latter is generated by deterministic rules, diffusion properties can be investigated analytically using tools from random walk theory on directed graphs [20]. In both cases, random walks through such structures are naturally correlated, due to the long jumps induced by the underlying self similar

topology.

The present work aims at understanding transport in this class of finite systems. This is a relevant issue for the interpretation of experiments, that typically deal with transport through finite samples (e.g. slabs) [4]. In the framework of random walk theory much progress has been made in the last years in the characterization of superdiffusive motion in infinite domains [21, 1]. On the other hand, the case of finite systems is relatively less developed [22, 23, 24, 25, 26, 27, 28]. The focus here will be on both stationary transport and time-dependent transmission for finite, one-dimensional structures. The study will be undertaken by means of a formulation in terms of a master equation for the process. This has several advantages for the theoretical analysis, since it deals directly with probabilities instead of ensembles of individual trajectories.

For quenched disorder, it is known that different averaging procedures [29] leads to different results. For the present class of models this requires for instance to distinguish among the possible types of initial conditions [17, 20]. In general, the averaging over an ensemble of trajectories still depends on the realization of the disorder. In particular, despite the walker is unbiased, for each single realization there may be a non-zero drift due to the intrinsic asymmetry of each specific arrangement of the scattering sites. For finite systems, this average drift is particularly important for characterizing the transmission properties of individual samples. Indeed, there may be cases in which the drift motion over the observational time is of the same order of the average diffusive spreading, thus affecting substantially the measurements. In the second part of the paper we will address this question by examining the scaling behavior of such drift and its statistics.

The paper is organized as follows. In section 2 we recall the definition of the model and its dynamics. In Section 3 we discuss the transport properties of a finite lattice under stationary conditions, i.e. when a constant flux of particles is kept at one side of the system. In this case, the models allows for analytic calculations. Then, in section 4 we turn to the time-resolved problem, namely to the situation in which particles are injected only at initial time at one lattice boundary. The related issue of the average drift induced by the statistical fluctuations of the structure in the random case is addressed in section 5.

## 2. The model

We consider a discrete-time random walk on a one-dimensional lattice. When the walker arrives at the  $n$ th site it can be transmitted with probability  $T_n$  (and reflected with probability  $R_n = 1 - T_n$ ). Clearly, the speed is conserved during the evolution and we can set its value to unity without loss of generality. Two types of sites are represented, the “transparent” ones for which  $T = 1$  that correspond to a completely ballistic propagation and the “scattering” ones, where  $T_n = T$ , ( $0 < T < 1$ ). In the

following we set  $T = 1/2$ , as the results are expected not to be affected by this choice up to inessential prefactors [30].

### 2.1. The Master Equation

The master equation of a random walker on one-dimensional lattice, accordingly with Persistent Random Walk model, is

$$p_n^+(t+1) = T_{n-1}p_{n-1}^+(t) + R_{n-1}p_{n-1}^-(t) \quad (1)$$

$$p_n^-(t+1) = R_{n+1}p_{n+1}^+(t) + T_{n+1}p_{n+1}^-(t) \quad (2)$$

where  $p_n^\pm$  is the walker’s probability to land at site  $n$  with positive velocity from the left side (+), or with negative velocity from the right side (−), so the total probability is  $p_n(t) = p_n^+(t) + p_n^-(t)$ . In this formulation, our model can be regarded as a random walk with a site-dependent persistence (see e.g. [31] and references therein).

### 2.2. The random and deterministic correlated Lévy Structures

We model correlated media in which the scatterers are distributed on a self similar set, such that the regions of ballistic sites are distributed according to a fat-tail. We will consider two classes of models (see fig.1). The first is random and has been first introduced in [17] (see also [18] and [20]). Here, the probability  $\lambda(r)$  to have two consecutive scattering sites separated by  $r$  ballistic ones is

$$\lambda(r) \equiv \frac{a}{r^{1+\alpha}}, \quad (3)$$

where  $\alpha > 0$ ,  $r$  is a positive integer and  $a$  a suitable normalization constant. Different realizations of the structure can be easily generated via a non-uniform random variate algorithm described in [32].

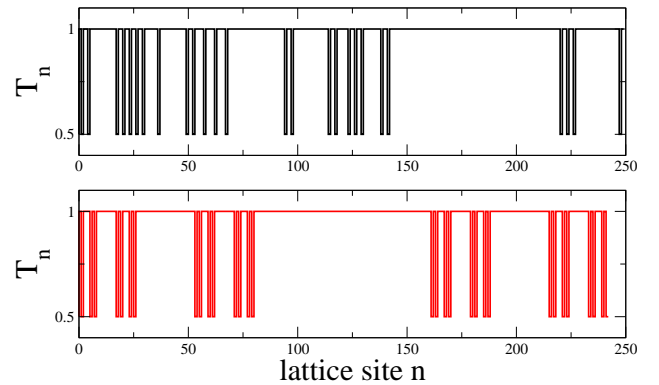


Figure 1: Illustration of the structures: transmission coefficient profiles  $T_n$  for the random (upper panel) and Cantor (lower panel) cases;  $\alpha = 0.630930$  corresponding to  $n_r = 2$ ,  $n_u = 3$ .

The second type is a class of deterministic quasi-lattices (see again fig.1), built by placing the scatterers on generalized Cantor sets [19]. Each sample, and the ensuing step length distribution, is defined by two parameters,  $n_u$  and

$n_r$ , used in its recursive construction. The former represents the growth of the longest step when the structures is increased by a generation, so that the longest step in a structure of generation  $G$  is proportional to  $n_u^G$ ;  $n_r$  is the number of copies of generation  $G - 1$  that form the generation  $G$ , so that the total number of scatterers in the generation  $G$  is proportional to  $n_r^G$  (see [19] for details). For this class of structures, the role of the exponent  $\alpha$  of the random case is played by  $\alpha = \log n_r / \log n_u$  [19]. Moreover, it can be shown that if  $n_u < n_r$  (i.e.  $\alpha > 1$ ) the fraction of scattering sites remains strictly positive in the thermodynamic limit  $G \rightarrow \infty$ . Thus we will refer to such a case as to the so called *fat* fractals. An example of this kind of structure is the Smith-Volterra-Cantor set. Conversely, we will name *slim* fractals the graphs with  $n_u > n_r$  (i.e.  $\alpha < 1$ ), where the measure of the scattering region is vanishing.

### 2.3. The Boundary conditions

In this work we are interested in finite lattices of a fixed number of sites, labeled by the integer  $n$  with  $n = 1, \dots, N$ . We thus need to specify the boundary conditions, by fixing the values of the probabilities on the 0th site on the left side ( $L$ ) and  $N + 1$ th site on the right side ( $R$ ). Let us define the probabilities on these sites  $p_0^\pm = p_L^\pm$  and  $p_{N+1}^\pm = p_R^\pm$ , so that:

$$p_L = p_L^+ + p_L^-, \quad p_R = p_R^+ + p_R^- \quad (4)$$

We also need to specify the currents at the system boundaries. To this aim let us consider the total probability

$$p_{TOT}(t) = \sum_{n=1}^N [p_n^+(t) + p_n^-(t)] \quad (5)$$

and using the master equation (2) we can write the continuity equation

$$p_{TOT}(t+1) = p_{TOT}(t) + J_L + J_R, \quad (6)$$

where we define

$$J_L \equiv R_0 p_0^- + T_0 p_0^+ - R_1 p_1^+ - T_1 p_1^- \quad (7)$$

$$J_R \equiv R_{N+1} p_{N+1}^+ + T_{N+1} p_{N+1}^- - R_N p_N^- - T_N p_N^+ \quad (8)$$

In the following we will compare two different cases:

*Mixed boundary conditions* where we impose a total reflection on the left side and an absorbing condition on the right,

$$J_L = 0, \quad p_0^+ = 0, \quad p_{N+1}^+ = 0, \quad p_{N+1}^- = 0. \quad (9)$$

Substituting (9) in (7) and (8) we obtain

$$R_0 p_0^- = R_1 p_1^+ + T_1 p_1^- \quad (10)$$

and the flux on the right side is

$$J_R = -R_N p_N^- - T_N p_N^+. \quad (11)$$

*Absorbing boundary conditions*, defined as

$$p_0^- = 0, \quad p_0^+ = 0, \quad p_{N+1}^+ = 0, \quad p_{N+1}^- = 0. \quad (12)$$

In this case, equations (7) e (8) reads:

$$J_L = -R_1 p_1^+ - T_1 p_1^- \quad (13)$$

and

$$J_R = -R_N p_N^- - T_N p_N^+. \quad (14)$$

### 3. The Stationary solution

Let us consider the time-independent solution of (2) on a finite lattice. It can be shown that such solution is obtained by transfer matrix method

$$\begin{pmatrix} p_{n+1}^+ \\ p_{n+1}^- \end{pmatrix} = \begin{pmatrix} T_n & R_n \\ -\frac{R_{n+1}T_n}{T_{n+1}} & \frac{1-R_nR_{n+1}}{T_{n+1}} \end{pmatrix} \begin{pmatrix} p_n^+ \\ p_n^- \end{pmatrix}, \quad (15)$$

and using boundary conditions, we can write the general form of equation (15)

$$\begin{pmatrix} p_R^+ \\ p_R^- \end{pmatrix} = \begin{pmatrix} m_{11} & m_{12} \\ m_{21} & m_{22} \end{pmatrix} \begin{pmatrix} p_L^+ \\ p_L^- \end{pmatrix} = M \begin{pmatrix} p_L^+ \\ p_L^- \end{pmatrix}, \quad (16)$$

where the  $2 \times 2$  matrix  $M$  is the product of  $N + 1$  transfer matrixes, Using equation (4) we have also

$$J_L = p_L^+ - p_L^-, \quad J_R = p_R^+ - p_R^- \quad (17)$$

and it is possible to evaluate the output flux  $J_R = J_L = J$ .

The matrix  $M$  is computed conveniently distinguishing between scattering and transparent sites. Obviously, for ballistic sites the associated matrix is the identity. For a block of  $s$  consecutive scattering sites the transfer matrix is

$$\begin{aligned} B_s &= \begin{pmatrix} T & R \\ 0 & 1 \end{pmatrix} \begin{pmatrix} T & R \\ -R & 2-T \end{pmatrix}^{s-1} \begin{pmatrix} 1 & 0 \\ -\frac{R}{T} & \frac{1}{T} \end{pmatrix} = \\ &= \begin{pmatrix} 1 - s\frac{R}{T} & s\frac{R}{T} \\ -s\frac{R}{T} & 1 + s\frac{R}{T} \end{pmatrix}, \end{aligned} \quad (18)$$

where we have used the matrix identity ( $n$  positive integer)

$$\begin{pmatrix} T & R \\ -R & 1+R \end{pmatrix}^n = \begin{pmatrix} 1-nR & nR \\ -nR & 1+nR \end{pmatrix} \quad (19)$$

If there are  $m$  equal blocks in the lattice  $1 \dots N$ , the total transfer matrix is the product of  $m$  times  $B_s$ , namely

$$M = B_s^m = \begin{pmatrix} 1 - ms\frac{R}{T} & ms\frac{R}{T} \\ -ms\frac{R}{T} & 1 + ms\frac{R}{T} \end{pmatrix}. \quad (20)$$

For the Cantor model at generation  $G$  the number of consecutive scatterers  $N_b = 2n_r^G$ , where  $n_r$  is the number of replicas. where  $ms = 2n_r^G$ . Resolving the system and using (4), (17) we obtain

$$J = -\frac{T}{4n_r^G R} (p_R - p_L) = -\frac{T}{4n_r^G R} \frac{\Delta p}{\Delta x} N \quad (21)$$

where  $\frac{\Delta p}{\Delta x}$  is the one-dimensional probability gradient. Using the first Fick's law we can write

$$D = \frac{N}{4n_r^G \frac{R}{T}} \quad (22)$$

For the random model we assume that there are  $m$  subsystem composed by only one ( $s = 1$ ) scattering site separated by a random distance  $l$  with a power-law distribution  $l^{-1-\alpha}$ . Similarly to the Cantor model, using (4) e (17) we obtain

$$J = -\frac{T}{2mR}(p_R - p_L) = -\frac{T}{2mR}\frac{\Delta p}{\Delta x}N \quad (23)$$

and the diffusion constant

$$D = \frac{N}{2m\frac{R}{T}} \quad (24)$$

The problem is thus to determine the statistics of the random variable  $m$  for fixed  $N$ . This is a nontrivial problem [18]. A simple estimate can be obtained as follows. Since  $N/m$  is the average distance between two consecutive scatterers we can write

$$\frac{N}{m} = \sum_{l=0}^N l^{-\alpha} \simeq \int_0^N l^{-\alpha} dl = \frac{N^{1-\alpha}}{1-\alpha} \quad (25)$$

and so we obtain

$$D = \frac{N^{1-\alpha}T}{2[1-\alpha]R} \quad (26)$$

Notice that the diffusion constant is proportional to  $T/R$  and it is finite for  $\alpha > 1$  and diverging for  $\alpha < 1$ . This is consistent with the results for the infinite domain [19, 20].

#### 4. Time-resolved transmission

Let us now turn to the case of time-resolved transmission. The type of experiment we have in mind is the following: an input pulse is applied at one boundary of the system and the output at the other side is observed. Some relevant prediction can be obtained by scaling arguments. The main quantity to consider is the probability for a walker to be at time  $t$  at distance  $r$  from the starting point, which we denote by  $p(r, t)$ . To investigate its dependence sample size, we consider its dynamical scaling properties.

The dynamical scaling hypothesis amounts to the fact that, on infinite domains, the evolution mostly depends on a single scaling length  $\ell(t)$ . More precisely [19, 20]  $p(r, t)$  can be written in scaling form as:

$$p(r, t) = \frac{1}{\ell(t)} f\left(\frac{r}{\ell(t)}\right), \quad (27)$$

for the random model and as:

$$p(r, t) = \frac{1}{\ell(t)} f\left[\frac{r}{\ell(t)}, g[\log_{n_u} \ell(t)]\right] \quad (28)$$

for the deterministic Cantor samples, with  $g$  periodic function (of unit period) accounting for log-periodic oscillations on the deterministic self-similar structures [20]. In the random case, the scaling function (27) can also present a subleading (i.e. vanishing in probability) term that can influence the evaluation of high order moments [19]. The scaling information is actually given by the growth law of the scaling length, which is predicted to be:

$$\ell(t) \sim \begin{cases} t^{\frac{1}{1+\alpha}} & \text{if } 0 < \alpha < 1 \\ t^{\frac{1}{2}} & \text{if } 1 \leq \alpha \end{cases} \quad (29)$$

Let us now turn to finite lattices of  $N$  sites, and estimate the size dependence from the scaling form. For walkers starting at time  $t = 0$  from the left border we consider the time-resolved transmitted current  $J_R(t, N)$ . Using the above scaling hypotheses one would argue that, at leading order, for  $\alpha < 1$ ,  $J_R(t, N) = B(N)G(t/N^{1+\alpha})$  where  $G(\cdot)$  is a scaling function. The coefficient  $B$  can be estimated as follows. The time-integrated current  $\int_0^\infty J_R(t, L)dt$  is by definition the total number of walkers escaping from the rightmost boundary. This, in turn, must be proportional to the conductivity, i.e. to  $N^{-\alpha}$  in the case of absorbing boundary conditions, and to 1 for the mixed ones (all the particles exit from the rightmost side in this case). A straightforward calculation thus yields

$$J_R(t, N) = \frac{1}{N^{1+\alpha}} G\left(\frac{t}{N^{1+\alpha}}\right) \quad (30)$$

for mixed boundary conditions, and

$$J_R(t, N) = \frac{1}{N^{1+2\alpha}} G\left(\frac{t}{N^{1+\alpha}}\right) \quad (31)$$

for absorbing conditions. For the case  $\alpha > 1$  a similar reasoning leads to the result

$$J_R(t, N) = \frac{1}{N^2} G\left(\frac{t}{N^2}\right) \quad (32)$$

for mixed boundary conditions, and

$$J_R(t, N) = \frac{1}{N^3} G\left(\frac{t}{N^2}\right) \quad (33)$$

for absorbing conditions.

The above prediction have been tested by solving iteratively the master equation (2) for lattices of different sizes  $N$  and for both mixed and absorbing boundary conditions. The initial condition is impulsive on the first site of the chain,  $p_{n,1}^\pm(0) = \frac{\delta_{1,n}}{2}$ . In fig. 2 and 3 we report the results for Cantor and the random model for different boundary conditions. An issue here concerns the sampling of disorder realizations. In the process of generating such realization it is often the case that some of them are devoided of scattering sites (except for the  $n = 1$  one that we always fix to have  $T_1 = 1/2$ ). Such realizations will affect the ensemble-averages via large ballistic peaks that hinder

a meaningful comparison with the expected theoretical estimates. We thus decided to cutoff the distribution  $\lambda$  up to some  $r_{max} \sim N$ , meaning that we consider only realizations where there is a minimal number of scatterers. This anyhow ensures that the scaling test is significant as  $N \rightarrow \infty$ . As seen in fig. 3 the data averaged of such ensemble nicely obey the expected scaling for both types of boundary conditions.

## 5. The average drift and its fluctuations in the random model

The class of system we are dealing with are characterized by a quenched disorder, so that the local transmission rates are fixed and are independent of time. Despite that the walker is unbiased, for each single realization there may be a nonzero average displacement, due to the intrinsic asymmetry of each specific realization of the system (see for instance the upper panel of fig. 1). In this section we aim at characterizing such a displacement and its sample-to-sample fluctuations. The main observables of interest we considered are the moments:

$$x_q = \left\langle \left| \sum_{n=1}^N (n - n_0) p_n(t) \right|^q \right\rangle = \langle |x_B|^q \rangle \quad (34)$$

Notice that the definition implies an average over trajectories and a further average over realization of the random structure, denoted by  $\langle \dots \rangle$ . The variable  $x_B = \sum_{n=1}^N (n - n_0) p_n(t)$  denotes the average position of the walker or the baricenter of the probability distribution, in a single disorder realization. Of course, as the structures are statistically symmetric under spatial reflection, the absolute value in the definition (34) is crucial to yield a nonzero ensemble average. The moments are assumed to grow asymptotically as  $x_q \sim t^{\gamma(q)}$ . The fact that  $\gamma(q)$  will be a nontrivial function of  $q$  it is a signature of the so-called strongly anomalous diffusion [33].

The behavior of the moments of  $x_B$  can be inferred as follows. In a disorder realization, let us consider the first  $n$  scattering sites placed to the right and to the left with respect  $x = 0$ , that denotes the scatterer corresponding to the starting point of the random walk. The positions of the  $n$  scatterers are  $X_{\pm n} = \pm \sum_{j=1}^n r_j^{\pm}$  where  $r_j^{\pm}$  are integers extracted from the spacing distributions  $\lambda(r)$ . The baricenter  $B$  of the region between  $X_n$  and  $X_{-n}$  is therefore  $B = \frac{X_n - X_{-n}}{2} = \frac{1}{2}(\sum_{j=1}^n r_j^+ - \sum_{j=1}^n r_j^-)$ . The distribution of the baricenters  $B$  over the disorder realization is given by:

$$P_B(B, n) = \int \prod_{j=1}^n \theta(r_j^+ - 1) \theta(r_j^- - 1) \lambda(r_j^+) \lambda(r_j^-) \delta \left( B - \frac{1}{2} \sum_{j=1}^n r_j^+ + \frac{1}{2} \sum_{j=1}^n r_j^- \right) dr_j^+ dr_j^- \quad (35)$$

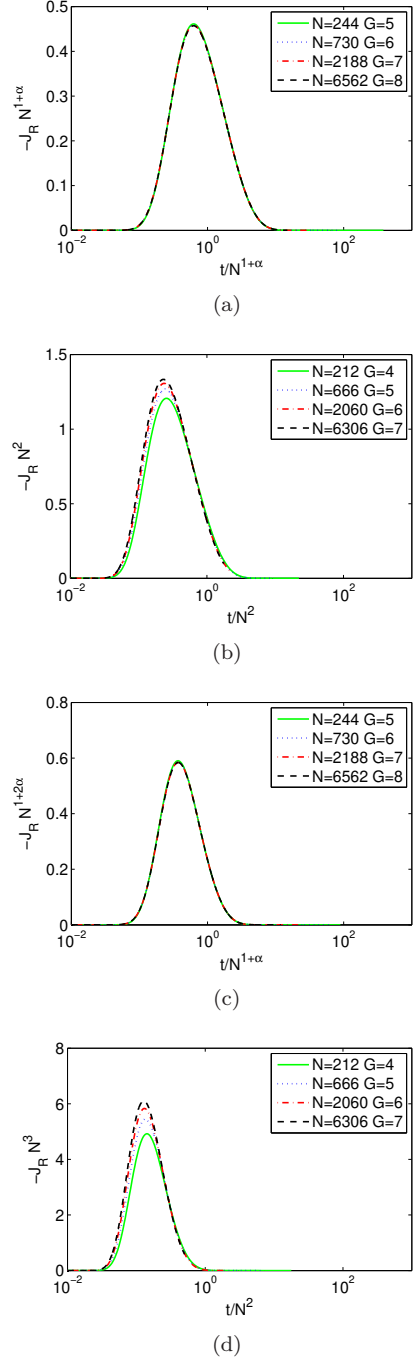


Figure 2: Cantor model: dynamic scaling of  $J_R(t, N)$  for different system sizes  $N$ : slim Cantor structure (a) and (c) ( $n_r = 2$ ,  $n_u = 3$  corresponding to  $\alpha = 0.630930$ ) and fat Cantor structure (b) and (d) ( $n_r = 3$ ,  $n_u = 2$  corresponding to  $\alpha = 1.584963$ ) with mixed boundary conditions and absorbing conditions respectively.



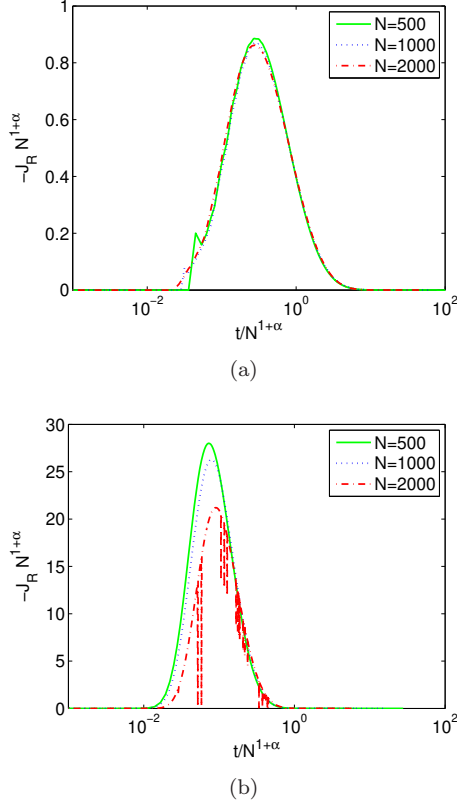


Figure 3: Random model: dynamic scaling of  $J_R(t, N)$  with mixed boundary conditions averaged on about 500 realizations of disorder and  $\alpha = 0.5$ : in fig. (a) the average of  $J_R(t)$  is obtained with all random configurations, on the other hand in fig. (b) the average is obtained removing the configurations having no or very few scattering sites (see text).

where the sum over the positions  $r_j^\pm$  has been replaced by an integral with a cutoff in  $r_j^\pm = 1$ . In the simpler case  $\alpha > 2$ , the process is diffusive and the probability that a walker has reached the  $n$ -th scattering site is  $p(n, t) \sim t^{-1/2} \exp(-n^2/(Ct))$ , where  $C$  is a suitable constant. We assume that, after averaging over the walk realizations, the sites between  $X_n$  and  $X_{-n}$  are visited uniformly. In this framework the average position of the walker in a certain disorder realization is given by  $x_B = \frac{X_n - X_{-n}}{2} = B$ . In particular, the distribution of  $x_B$  at time  $t$  is:

$$P(x_B, t) \sim t^{-1/2} \int e^{-n^2/(Ct)} P_B(x_B, n) dn \quad (36)$$

where again we replace the sum over  $n$  with an integral. Taking the Fourier transform with respect  $x_B$  one obtains

$$\tilde{P}(k_B, t) \sim t^{-1/2} \int e^{-n^2/(Ct)} \left( \tilde{\lambda}(k_B/2) \tilde{\lambda}(-k_B/2) \right)^n dn \quad (37)$$

where  $\tilde{\lambda}(k)$  is the Fourier transform of  $\lambda(r)$ . Since we are interested in the asymptotic behavior at large  $x_B$  (i.e. at small  $k_B$ ), we get, for  $\alpha > 2$ ,  $\tilde{\lambda}(k) \simeq 1 + ik_B \langle r \rangle - k^2 \langle r^2 \rangle / 2$  and then  $\tilde{\lambda}(k) \tilde{\lambda}(-k) \simeq 1 - k^2 (\langle r^2 \rangle - \langle r \rangle^2) \simeq \exp(-k^2 \Delta_r^2)$ . Plunging this expression into Eq. (37) we have

$$\tilde{P}(k_B, t) \sim t^{-1/2} \int e^{-n^2/(Ct)} e^{-k_B^2 n \Delta_r^2 / 4} dn. \quad (38)$$

Eq. (38) entails that  $\tilde{P}(k_B, t) = \tilde{f}(k_B/t^{1/4})$  or equivalently  $P(k_B, t) = t^{-1/4} f(k_B/t^{1/4})$  where  $\tilde{f}(\cdot)$  and  $f(\cdot)$  are suitable scaling function. Notice that the scaling length of the process grows as  $\ell_B(t) \sim t^{1/4}$  [29].

For  $1 < \alpha < 2$ , the same calculation holds up to Eq. (37), as the process is diffusive also in this case. However, now the fluctuations of  $\lambda(r)$  are diverging, hence we obtain at small  $k$   $\tilde{\lambda}(k) \simeq 1 + ik_B \langle r \rangle - D_1 |k|^\alpha$  and  $\tilde{\lambda}(k) \tilde{\lambda}(-k) \simeq \exp(-D_1^2 |k|^{2\alpha})$ , where  $D_1$  is a suitable constant. Then, analogously to the previous case we have

$$\tilde{P}(k_B, t) \sim t^{-1/2} \int e^{-n^2/(Ct)} e^{-D_1^2 k_B^{2\alpha} n / 4} dn. \quad (39)$$

From Eq. (39) we get that the scaling form of the probability distribution is  $\tilde{P}(k_B, t) = \tilde{f}(k_B/t^{1/(2\alpha)})$ , i.e.  $P(k_B, t) = t^{-1/(2\alpha)} f(k_B/t^{1/(2\alpha)})$  and  $\ell_B(t) \sim t^{1/(2\alpha)}$ .

Finally, for  $\alpha < 1$  the process is not diffusive and  $p(n, t)$  is not Gaussian. However, one can estimate how many different scattering sites the walker encounters in a time  $t$ . First, the number of scattering sites within a distance  $\ell$  from the starting point grows as  $n \sim \ell^\alpha$  [18]; then, ignoring rare long jump events, the typical distance covered by a walker in a time  $t$  is  $\ell(t) \sim t^{1/(\alpha+1)}$  [20]. Hence we get  $n(t) \sim t^{\alpha/(\alpha+1)}$ . Therefore, we expect that  $p(n, t)$  satisfies the scaling form  $p(n, t) \sim t^{-\alpha/(\alpha+1)} g(n/t^{\alpha/(\alpha+1)})$  where  $g(\cdot)$  is a suitable scaling function. In the approximation of a uniform exploration of the interval  $[X_n X_{-n}]$  we obtain the analogous of Eq. 36; i.e.

$$P(x_B, t) \sim t^{-\alpha/(1+\alpha)} \int g\left(\frac{n}{t^{\alpha/(1+\alpha)}}\right) P_B(x_B, n) dn. \quad (40)$$

Now the first moment of  $\lambda(r)$  diverges and we have  $\tilde{\lambda}(k) \simeq 1 - D_2|k|^\alpha$  and  $\tilde{\lambda}(k)\tilde{\lambda}(-k) \simeq \exp(-2D_1|k|^\alpha)$ . Analogously to Eq. 39, we get for the Fourier transform:

$$\tilde{P}(k_B, t) \sim t^{-\alpha/(1+\alpha)} \int \left( \frac{n}{t^{\alpha/(1+\alpha)}} \right) e^{-2D_1 n|k_B|^\alpha} dn. \quad (41)$$

which implies that the scaling form is  $P(x_B, t) = t^{-1/(1+\alpha)} f(x_B/t^{1/(1+\alpha)})$  with  $\ell_B(t) \sim t^{1/(1+\alpha)}$

Therefore in the different  $\alpha$  regimes the scaling length  $\ell_B(t)$  governing the dynamics of the baricenter  $x_B$  is:

$$\ell_B(t) = \begin{cases} t^{1/4} & \text{for } \alpha > 2 \\ t^{1/(2\alpha)} & \text{for } 1 < \alpha < 2 \\ t^{1/(1+\alpha)} & \text{for } \alpha < 1 \end{cases} \quad (42)$$

Comparing  $\ell_B(t)$  with the scaling length  $\ell(t)$  (29), obtained by averaging both over the disorder and the random walks realizations, we get that  $\ell_B(t)$  is subleading for  $\alpha > 1$ , while the two scaling lengths are of the same order of magnitude for  $\alpha < 1$ . This means that, for  $\alpha > 1$  the fluctuations due to random walks dynamics are much larger than the fluctuations due to the different realization of the disorder. The latter, therefore, are very difficult to measure, for example observing the probability distribution of a walker in a single disorder realization  $p_n(t)$ . On the other hand, for  $\alpha < 1$  the distribution  $p_n(t)$  should display distortions due to the disorder realization which are of the same magnitude of  $\ell(t)$  i.e. the typical size of  $p_n(t)$  and therefore they should be more easily observed in experiments.

If the dynamics does not present strong anomalous features, the moments of  $\langle x_B^q \rangle$  can be directly evaluated as  $\ell_B(t)^q$ . However, when the spacing between the scattering events are characterized by power laws, jumps much larger than the scaling length are not exponentially suppressed and this can give rise to a long tail  $h(x_B, t)$  in the distribution  $P(x_B, t)$ . The tail  $h(x_B, t)$  provides a non trivial contribution to the high order moments, modifying the value of the exponent  $\gamma(q)$  and giving rise to strongly anomalous diffusion. In particular,  $\gamma(q)$  can be evaluated by means of a single long jump approach [19, 20]. We remark that a jump much larger than the scaling length affects in the same way the process averaged over the disorder and the single disorder realization. In particular, the probability of a long jump can be evaluated as  $h(x_B, t) \sim N(t)\lambda(x_B)$ , where  $\lambda(x_B)$  is the probability that one of the segment between scatterers is of length  $x_B$ , and  $N(t)$  is the number of scatterer visited by the walker in a time  $t$ . Therefore we obtain for the single long jump mechanism the same exponents already evaluated in [19, 20]. In particular, the contribution to the moment  $\langle x_B^q \rangle$  grows as  $t^{q+0.5-\alpha}$  if  $\alpha > 1$  and  $t^{q-\alpha^2/(1+\alpha)}$  if  $\alpha < 1$ . Comparing these behaviors with the contribution to  $\langle x_B^q \rangle$  obtained in the scaling approach

i.e.  $\ell_B(t)^q$  we get the complete picture for  $\gamma(q)$

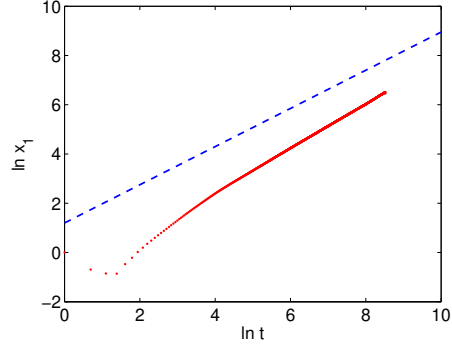
$$\begin{aligned} \text{for } \alpha > 2 \quad \gamma(q) &= \begin{cases} \frac{q}{4} & \text{for } q < \frac{4}{3}\alpha - \frac{2}{3} \\ \frac{1}{2} + q - \alpha & \text{otherwise} \end{cases} \\ \text{for } 1 < \alpha < 2 \quad \gamma(q) &= \begin{cases} \frac{q}{2\alpha} & \text{for } q < \alpha \\ \frac{1}{2} + q - \alpha & \text{otherwise} \end{cases} \\ \text{for } \alpha < 1 \quad \gamma(q) &= \begin{cases} \frac{q}{1+\alpha} & \text{for } q < \alpha \\ \frac{q(1+\alpha)-\alpha^2}{1+\alpha} & \text{otherwise} \end{cases} \end{aligned} \quad (43)$$

In fig. 4 the time-evolution of  $x_1$  in double-logarithmic scale for the three cases  $\alpha = 0.6$ ,  $\alpha = 1.5$  and  $\alpha = 3.0$ . In order to avoid any boundary effect, the structures have been generated by growing two different lattices each of length  $N/2$  around the initial site  $n_0$  and considering times shorter than  $N/2$ . Another important limitation for the numerical test regards the time range where the predicted scaling is expected to be observable for higher-order moments. To have a sufficient sampling one needs to consider a number of realizations with a significative number of jumps much larger of  $\ell_B(t)$ . For  $\alpha > 2$ , the probability of obtaining one of this jumps decays with time as  $\int_{\ell_B(t)}^\infty h(y, t) dy \sim t^{(2-\alpha)/4}$ , i.e. for  $\alpha < 2$  the tail  $h(x_B, t)$  is subleading with respect to  $P_B(x_B, t)$  for large times. So the number of realizations needed to observe single long jumps grows as  $t^{(\alpha-2)/4}$  and this means that the time-range which can be employed to measure the exponents is bounded from above. If we take into account this limitation, we can reliably extract the exponent from the available data. fig. 5 shows that, up to the statistical accuracy the data are in excellent agreement with the analytical estimates.

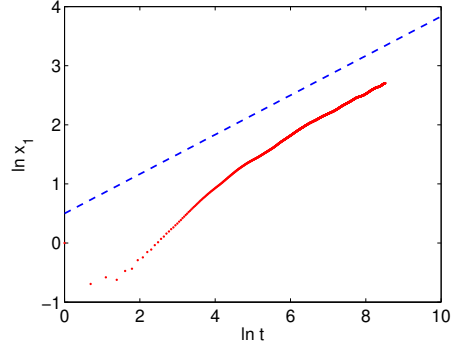
## 6. Conclusions

We have studied stationary and time-dependent transmission of walkers through finite one-dimensional lattice where scatterers are arranged on random and deterministic self similar structures with Lévy distributed disorder. Using scaling arguments we have predicted the dependence of particle currents on  $N$  that have been successfully tested against the solution of the associated master equation. The latter approach has considerable advantages with respect to direct Monte Carlo simulations of the random walk as it allows to obtain averages over trajectories ensembles without the statistical errors. Altogether the results nicely fit into the global picture that emerged from the recent literature [18, 19, 20]. Although we focused on one-dimensional structures only, most of the results carry over to the case of higher-dimensional samples like  $2d$  and  $3d$  Lévy glasses [34, 16] which are of course of major experimental relevance.

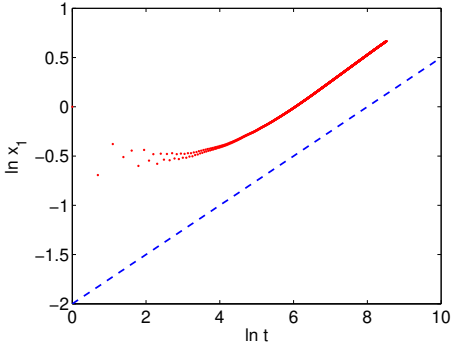
A related question we addressed is the problem of the average drift on a specific realization. We demonstrated that the scaling arguments are of help to understand quantitatively also this issue. In particular, we showed that



(a)  $\alpha = 0.6$

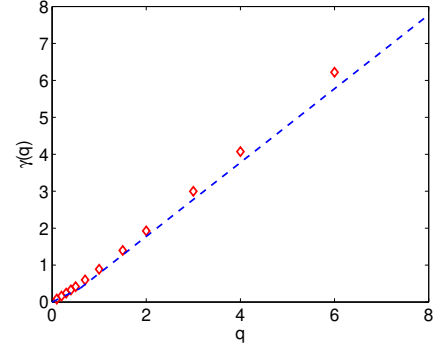


(b)  $\alpha = 1.5$

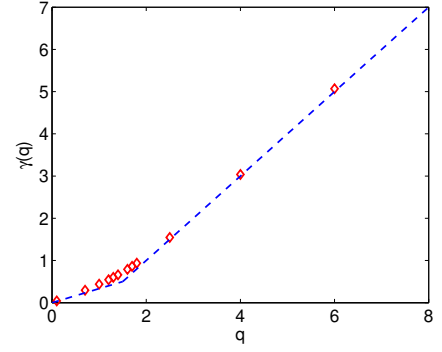


(c)  $\alpha = 3.0$

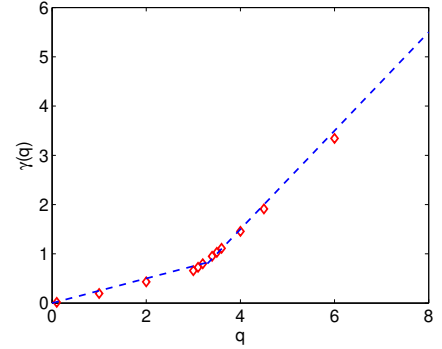
Figure 4: The moment  $x_1$  as defined by (34) for three values  $\alpha$ :  $\alpha = 0.6$  (a),  $\alpha = 1.5$  (b) e  $\alpha = 3.0$  (c); averages over 2000 realizations.



(a)  $\alpha = 0.6$



(b)  $\alpha = 1.5$



(c)  $\alpha = 3.0$

Figure 5: The scaling exponents  $\gamma(q)$  for three values of  $\alpha$ :  $\alpha = 0.6$  (a),  $\alpha = 1.5$  (b) e  $\alpha = 3.0$  (c). The exponent have been obtained by power-law fitting of  $x_q(t)$ ; averages are each over a few thousands realization of the structure.



when the disorder is characterized by a diverging average length of the spacings (i.e. for  $\alpha < 1$ ) an anomalous drift arises in the position of the baricenter of the probability distribution. Here, the fluctuations due to the different realization of the disorder are of the same magnitude of  $\ell(t)$  i.e. the typical size of  $p_n(t)$  and therefore they should be more easily observed in experiments.

## Acknowledgements

We acknowledge useful discussions with R. Livi.

## References

- [1] R. Klages, G. Radons, I. M. Sokolov (Eds.), *Anomalous Transport: Foundations and Applications*, Wiley-VCH Verlag, Weinheim, 2008.
- [2] P. E. Smouse, S. Focardi, P. R. Moorcroft, J. G. Kie, J. D. Forester, J. M. Morales, *Stochastic modelling of animal movement*, *Phil. Trans. R. Soc. B* 365 (1550) (2010) 2201–2211.
- [3] A. Baronchelli, F. Radicchi, *Lévy flights in human behavior and cognition*, *Chaos, Solitons & Fractals* 56 (2013) 101 – 105.
- [4] P. Barthelemy, J. Bertolotti, D. Wiersma, *A Lévy flight for light*, *Nature* 453 (7194) (2008) 495–498.
- [5] J. Bertolotti, K. Vynck, L. Pattelli, P. Barthelemy, S. Lepri, D. S. Wiersma, *Engineering Disorder in Superdiffusive Lévy Glasses*, *Advan. Func. Mat.* 20 (6) (2010) 965–968.
- [6] A. Blumen, G. Zumofen, J. Klafter, *Transport aspects in anomalous diffusion: Lévy walks*, *Phys. Rev. A* 40 (7) (1989) 3964–3973.
- [7] J. Klafter, A. Blumen, G. Zumofen, M. F. Shlesinger, *Lévy walk approach to anomalous diffusion*, *Physica A* 168 (1) (1990) 637–645.
- [8] T. Geisel, *Lévy walks in chaotic systems: Useful formulas and recent applications*, in: *Lévy flights and related topics in physics*, Springer, 1995, pp. 151–173.
- [9] T. Geisel, J. Nierwetberg, A. Zacherl, *Accelerated diffusion in josephson junctions and related chaotic systems*, *Phys. Rev. Lett.* 54 (7) (1985) 616–619.
- [10] P. Cipriani, S. Denisov, A. Politi, *From Anomalous Energy Diffusion to Lévy Walks and Heat Conductivity in One-Dimensional Systems*, *Phys. Rev. Lett.* 94 (24) (2005) 244301.
- [11] L. Delfini, S. Denisov, S. Lepri, R. Livi, P. K. Mohanty, A. Politi, *Energy diffusion in hard-point systems*, *Eur. Phys. J.-Special Topics* 146 (2007) 21–35.
- [12] R. Kutner, P. Maass, *Lévy flights with quenched noise amplitudes*, *J. Phys. A: Math. Gen.* 31 (11) (1998) 2603.
- [13] H. Fogedby, *Lévy flights in random environments*, *Phys. Rev. Lett.* 73 (19) (1994) 2517–2520.
- [14] M. Schulz, *Lévy flights in a quenched jump length field: a real space renormalization group approach*, *Phys. Lett. A* 298 (2-3) (2002) 105–108.
- [15] P. Barthelemy, J. Bertolotti, K. Vynck, S. Lepri, D. S. Wiersma, *Role of quenching on superdiffusive transport in two-dimensional random media*, *Phys. Rev. E* 82 (2010) 011101.
- [16] C. W. Groth, A. R. Akhmerov, C. W. J. Beenakker, *Transmission probability through a Lévy glass and comparison with a Lévy walk*, *Phys. Rev. E* 85 (2012) 021138.
- [17] E. Barkai, V. Fleurov, J. Klafter, *One-dimensional stochastic Lévy-Lorentz gas*, *Phys. Rev. E* 61 (2000) 1164–1169.
- [18] C. W. J. Beenakker, C. W. Groth, A. R. Akhmerov, *Nonalgebraic length dependence of transmission through a chain of barriers with a Lévy spacing distribution*, *Phys. Rev. B* 79 (2009) 024204.
- [19] R. Burioni, L. Caniparoli, S. Lepri, A. Vezzani, *Lévy-type diffusion on one-dimensional directed Cantor graphs*, *Phys. Rev. E* 81 (2010) 011127.
- [20] R. Burioni, L. Caniparoli, A. Vezzani, *Lévy walks and scaling in quenched disordered media*, *Phys. Rev. E* 81 (2010) 060101.
- [21] R. Metzler, J. Klafter, *The restaurant at the end of the random walk: recent developments in the description of anomalous transport by fractional dynamics*, *J. Phys A: Math. Gen.* 37 (31) (2004) R161.
- [22] A. Davis, A. Marshak, *Lévy kinetics in slab geometry: Scaling of transmission probability*, in: *Fractal Frontiers World Scientific*, Singapore, 1997, pp. 63–72.
- [23] P. M. Drysdale, P. A. Robinson, *Lévy random walks in finite systems*, *Phys. Rev. E* 58 (5) (1998) 5382–5394.
- [24] H. Larralde, F. Leyvraz, G. Martínez-Mekler, R. Rechtman, S. Ruffo, *Transmission and scattering of a lorentz gas on a slab*, *Phys. Rev. E* 58 (4) (1998) 4254.
- [25] S. V. Buldyrev, S. Havlin, A. Y. Kazakov, M. G. E. da Luz, E. P. Raposo, H. E. Stanley, G. M. Viswanathan, *Average time spent by Lévy flights and walks on an interval with absorbing boundaries*, *Phys. Rev. E* 64 (4) (2001) 041108.
- [26] B. P. van Milligen, I. Calvo, R. Sánchez, *Continuous time random walks in finite domains and general boundary conditions: some formal considerations*, *J. Phys. A: Math. Theor.* 41 (21) (2008) 215004.
- [27] S. Lepri, A. Politi, *Density profiles in open superdiffusive systems*, *Phys. Rev. E* 83 (3) (2011) 030107.
- [28] A. Dhar, K. Saito, B. Derrida, *Exact solution of a Lévy walk model for anomalous heat transport*, *Phys. Rev. E* 87 (2013) 010103.
- [29] J.-P. Bouchaud, A. Georges, *Anomalous diffusion in disordered media: Statistical mechanisms, models and physical applications*, *Phys. Rep.* 195 (4-5) (1990) 127–293.
- [30] R. Burioni, S. di Santo, S. Lepri, A. Vezzani, *Scattering lengths and universality in superdiffusive Lévy materials*, *Phys. Rev. E* 86 (2012) 031125.
- [31] M. Miri, Z. Sadjadi, M. E. Fouladvand, *Persistent random walk on a site-disordered one-dimensional lattice: Photon subdiffusion*, *Phys. Rev. E* 73 (3) (2006) 031115.
- [32] L. Devroye, *Non-Uniform Random Variate Generation*, Springer-Verlag, New York, 1986.
- [33] P. Castiglione, A. Mazzino, P. Muratore-Ginanneschi, A. Vulpiani, *On strong anomalous diffusion*, *Physica D* 134 (1) (1999) 75–93.
- [34] P. Buonsante, R. Burioni, and A. Vezzani, *Transport and scaling in quenched two- and three-dimensional Lévy quasicrystals*, *Phys. Rev. E* 84, (2011) 021105 .
- [35] R. Burioni, E. Ubaldi, and A. Vezzani, *Superdiffusion and transport in two-dimensional systems with Lévy-like quenched disorder*, *Phys. Rev. E* 89, (2014) 022135.